Removal of Erythrosine Dye from Aqueous Solutions using Mesoporous Silica Synthesised from Coal Bottom Ash

Afifah Athirah Saini¹, Anis Haziqah Mohd Yusof¹, Fatin Nur Athirah Mohmad Rosli¹, Muhamad Hafiz Zulkafli¹, Mursyida Mohd Dakroh¹, Maryam Husin¹ and Hamizah Md Rasid^{1,2}*

¹School of Chemistry and Environment, Faculty of Applied Sciences, Universiti Teknologi MARA, 40450 Shah Alam, Selangor, Malaysia

²Multifunctional Nanoporous Material Research Group, Universiti Teknologi MARA, Shah Alam, Malaysia *Corresponding author (e-mail: hamizah7708@uitm.edu.my)

In recent years, a large amount of coal bottom ash (CBA) has been generated as a by-product of coal-fired power plants and discharged into the environment, subsequently raising global concern and contributing to serious environmental burdens. Converting this thermal waste into more valuable products is highly desirable for global resource conservation and environmental sustainability. Due to its high silica content, CBA can serve as a silica source for synthesising a variety of porous materials. In this study, alkaline fusion was used to extract silica from CBA, and the resulting supernatant solution provided a silica source for synthesising mesoporous silica materials. Extensive characterisation of these materials was conducted using Fourier Transform Infrared (FTIR) Spectroscopy, Powder X-ray Diffraction (PXRD), and Scanning Electron Microscopy with Energy Dispersive X-ray Analysis (SEM-EDX) to identify the functional groups, crystalline phases, and surface morphology. The results indicated the presence of surface hydroxyl groups and symmetric Si-O stretching in the FTIR spectra, confirming the successful synthesis of mesoporous silica. The XRD patterns showed an ordered pore structure, while the EDX spectra identified silica and oxygen elements in the synthesised materials. Additionally, adsorption studies were performed to evaluate the potential of the synthesised mesoporous silica materials as adsorbents for removing erythrosine, a synthetic dye, from aqueous solutions. Preliminary results showed that the silica materials exhibited effective adsorption capacity for erythrosine, demonstrating their potential for environmental applications in dye removal. This approach demonstrates that using a low-cost silica source like CBA offers a promising pathway to transform coal waste into valuable products, potentially contributing to the industrial-scale production of porous materials for environmental cleanup.

Keywords: Coal bottom ash; mesoporous silica; erythrosine adsorption

Received: April 2025; Accepted: August 2025

Economic development and population growth are straining energy resources. Coal, the world's secondlargest energy source, accounts for nearly 30% of global primary energy consumption and is expected to remain a dominant electricity generation source for the foreseeable future [1]. During electricity generation, coal combustion produces coal fly ash (CFA) and coal bottom ash (CBA) as by-products [2]. In Malaysia, this results in approximately 6.8 million tonnes of CFA and 1.7 million tonnes of CBA annually [3]. Despite fly ash being widely recycled in the cement industry, bottom ash remains underutilised and is stored in ash ponds [4]. If not recycled, these ponds fill quickly, raising concerns about potential leachate and environmental impact [5]. Recognising industrial by-products as resources has spurred innovative recycling solutions [1].

In 1990, Mobil Corporation developed the M41S family of mesoporous silica materials, which

feature uniform pore distributions (2-50 nm), a high specific surface area (1000 m²/g), and excellent thermal and hydrothermal stability. These materials are widely used as catalysts for adsorbing organic compounds and removing heavy metals from wastewater [6]. However, the high cost of raw silica materials, derived from sodium silicates and tetraethyl orthosilicate (TEOS), limits their widespread application. CBA is rich in silica and offers a potential alternative to enhance recycling rates while lowering costs for mesoporous silica production. This silica can then be used as an effective adsorbent for environmental pollution control [6].

Erythrosine, a widely used food colouring agent, is of environmental concern due to its toxic effects. When discharged into industrial wastewater, erythrosine can contaminate water bodies and pose risks to human health and ecosystems. Among the impacts are endotoxic, mutagenic, and cytotoxic effects [7]. Given that 98% of water use relies on rivers, efficient removal of erythrosine is crucial.

18 Afifah Athirah Saini, Anis Haziqah Mohd Yusof, Fatin Nur Athirah Mohmad Rosli, Muhamad Hafiz Zulkafli, Mursyida Mohd Dakroh, Maryam Husin and Hamizah Md Rasid Removal of Erythrosine Dye from Aqueous Solutions using Mesoporous Silica Synthesised from Coal Bottom Ash

Adsorption is a highly effective method for removing such pollutants, with mesoporous silica emerging as a promising adsorbent due to its high capacity.

This study aims to extract silica from CBA and synthesise mesoporous silica materials for erythrosine removal from aqueous solutions. The materials were characterised using Fourier Transform Infrared Spectroscopy (FTIR), Powder X-ray Diffraction (PXRD), and Scanning Electron Microscopy with Energy Dispersive X-ray Analysis (SEM-EDX). The efficacy of these synthesised materials as adsorbents for erythrosine was also investigated.

EXPERIMENTAL

Extraction of Silica from CBA via the Alkali Fusion Method

The alkali fusion method, adapted from Chandrasekar et al. [8], was used to extract silica. Granular bottom ash was ground into fine powder using a mortar and pestle. The powder was mixed with sodium hydroxide (NaOH) in a 1:1.2 weight ratio and heated at 550 °C for 1 hour. The resulting products were cooled, ground into a fine powder, and mixed with distilled water in a 1:4 weight ratio. The mixture was stirred for 24 hours, then centrifuged and filtered. The supernatant served as the silica source for mesoporous silica synthesis.

Synthesis of Mesoporous Silica Materials

The synthesis followed the method of de Oliveira et al. [9]. A reaction mixture with a molar ratio of 1.0:0.25:0.08:103.5 (silicon oxide/NaOH/CTABr/H₂O) was prepared. First, 1.8 g of cetyltrimethylammonium bromide (CTABr) was dissolved in 40 mL of deionised water under magnetic stirring at 350 rpm for 30 minutes. Next, 37 mL of silica source was added, and stirring was continued for 2 hours. Afterwards, 2 mol/L of hydrochloric acid (HCl) was added and the solution was stirred for another 30 minutes until a gel (at pH 7, 9, or 11) or a clear solution (at pH 13) formed. The mixture was transferred to a Teflon-lined stainless-steel autoclave and heated at 110 °C for 24 hours under autogenous pressure. The resulting material was washed, dried at 110 °C for 12 hours, and calcined at 560 °C for 6 hours at a heating rate of 1 °C/min. After cooling, the samples were ground and sieved through 200-mesh sieves.

Characterisation of Mesoporous Silica Materials

Various characterisation techniques were used to assess the physicochemical properties and structure of the synthesised materials. FTIR was performed to identify organic and inorganic compounds. Each sample was mixed with potassium bromide (KBr) in a 1:9 ratio and ground into a homogeneous mixture, which was then pressed into pellets for analysis from $4000~\text{cm}^{-1}$ to $400~\text{cm}^{-1}$. PXRD was used to identify crystalline phases. A 20 mg sample was mounted and measured in the 20 range of 0° to 2°. SEM-EDX was employed to examine surface morphology. Each sample was coated with gold and examined at 3kV to 10kV for enhanced image quality.

Adsorption Studies

A 500 mg/L erythrosine stock solution was prepared by dissolving 0.5 g of erythrosine in 1 L of deionised water. Diluted solutions (20, 40, 60, 80, and 100 mg/L) were prepared by taking aliquots of 2, 4, 6, 8, and 10 mL from the stock solution and diluting them to 100 mL with distilled water. Adsorption studies were conducted to evaluate the effects of pH, dye initial concentration, and adsorbent dosage. In each experiment, 25 mL of dye solution was mixed with a specified amount of adsorbent (100 BSS mesh size). The flasks were agitated until equilibrium was reached, and the supernatant was filtered through Whatman filter paper (No. 41). Absorbance was measured at 526 nm. The removal efficiency (%) was calculated using the formula shown in Equation 1:

Removal efficiency (%) =
$$\frac{\text{Co-Ce}}{\text{Co}} \times 100\%$$
 (1)

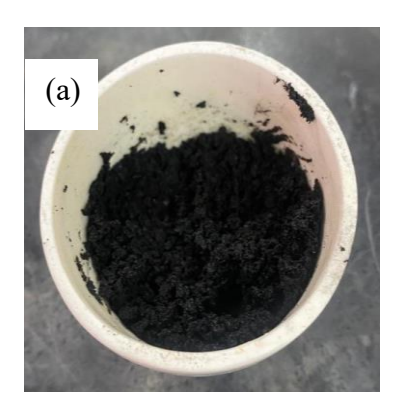
where C_0 is the initial concentration (mg/L) and C_e is the final concentration (mg/L).

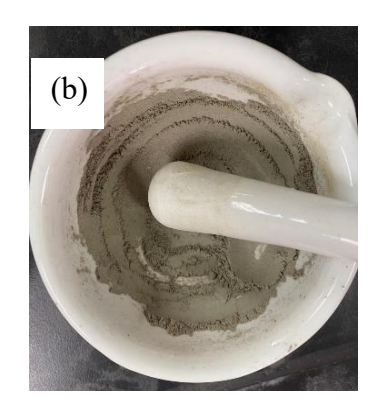
RESULTS AND DISCUSSION

The discussion is organised into three sections: extraction of silica from bottom ash, sample characterisation, and erythrosine adsorption study.

Extraction of Silica from Bottom Ash

Figure 1(a) shows CBA from the Tanjung Bin Power Plant in Pontian, Johor, Malaysia. The coarse bottom ash was ground into fine powder. Figure 1(b) shows the mixture of NaOH and ground bottom ash, which was fused in a furnace at 550 °C for 1 hour to extract silica. The alkali fusion method not only extracts silica but also removes impurities, such as heavy metals (Cu, Zn, and Pb), that could affect the colour and clarity of the solution [10]. As a result, the final product (i.e., the bottom ash supernatant) appeared as a clear white solution (see Figure 1(c)). This clarity indicates the successful removal of impurities during the extraction process and the successful extraction of silica via the alkali fusion method.





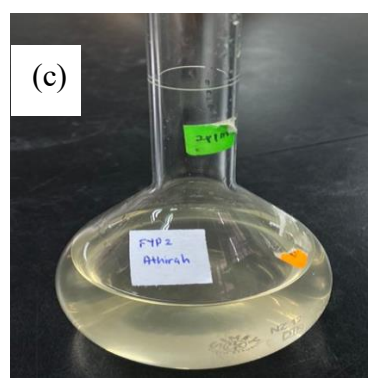


Figure 1. Images of (a) CBA, (b) mixture of powder CBA and NaOH, (c) bottom ash supernatant.

Table 1. Adsorption band (cm⁻¹) and band assignments.

Adsorption Band (cm ⁻¹)	Band Assignments	
3500	O-H stretching (adsorbed water)	
2850-3000	C-H stretching (alkyl group of surfactants in uncalcined samples)	
1600-1650	Deformation in hydroxyl groups	
1062.80-797.89	Asymmetric and symmetric Si-O-Si stretching (uncalcined)	
1080-798.68	Asymmetric and symmetric Si-O-Si stretching (calcined)	
466.05	Si-O bending (uncalcined)	
469.07-735.12	Si-O bending and stretching (calcined)	

Sample Characterisation

The FTIR spectra provide distinct molecular fingerprints based on vibrational modes, offering detailed information about the functional groups in synthesised mesoporous silica materials. Table 1 lists the adsorption bands and their assignments.

Figure 2 shows the FTIR spectra of the uncalcined and calcined samples. The broad band at 3500 cm⁻¹ in the calcined sample indicates surface silanol groups and adsorbed water [11]. The broadness of this band reflects the strength of hydrogen bonding between the hydroxyl groups of silanols and adsorbed water molecules. In the uncalcined sample, the peaks at 2850–3000 cm⁻¹ correspond to C-H stretching, attributed to the alkyl group of

surfactant molecules (CTABr). The absence of these peaks after calcination demonstrates that the surfactant had been completely removed.

The peak between 1600–1650 cm⁻¹ observed in both uncalcined and calcined samples is associated with the deformation of hydroxyl species on the surface [11]. The asymmetric and symmetric stretching vibration bands of Si-O-Si groups appeared at 1080.07 cm⁻¹ and 798.68 cm⁻¹ in the calcined samples and 1062.80 cm⁻¹ and 797.89 cm⁻¹ in the uncalcined sample. Peaks at 466.05 cm⁻¹ in spectrum (a) and 469.07 cm⁻¹ in spectrum (b) are attributed to bending vibrations, while the peak at 735.12 cm⁻¹ in spectrum (b) is related to the stretching vibration of Si-O species on the surface of mesoporous silica [9].

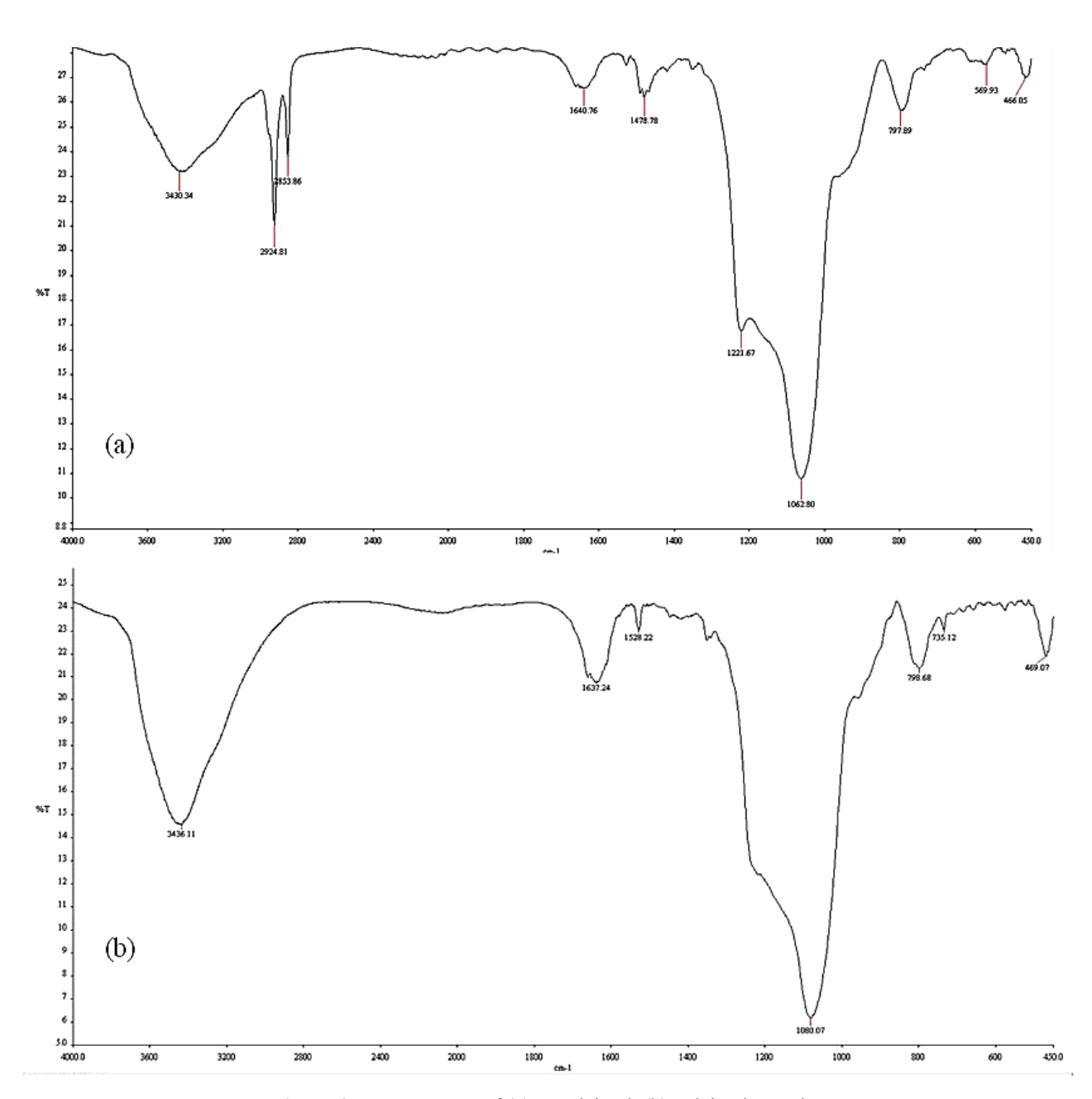
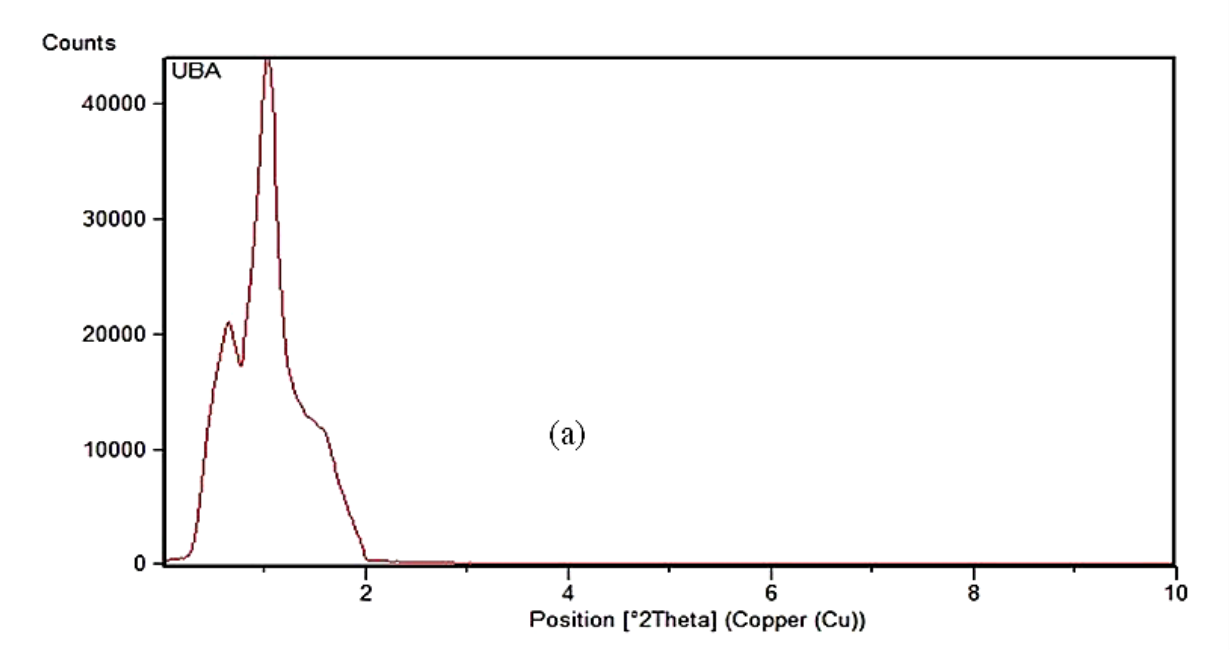


Figure 2. FTIR spectra of (a) uncalcined, (b) calcined sample.

Figure 3 shows the low-angle X-ray diffractograms of the uncalcined and calcined samples. The XRD pattern of both samples indicates a strong peak characteristic of the (100) plane, indicating a higher ordering of pore structure in the synthesised samples [12]. Weak diffraction peaks corresponding to the (110) and (200) planes were also observed for both uncalcined and calcined samples,

which are typical of the formation of an ordered pore structure and confirm the synthesis of mesoporous silica [9]. In comparison, the uncalcined samples exhibited a broad peak with lower intensity, while the peaks for the calcined samples were much stronger, narrower, and slightly shifted to a lower angle. This can be attributed to an increase in the interplanar spacing, indicating a rise in crystallinity [13].



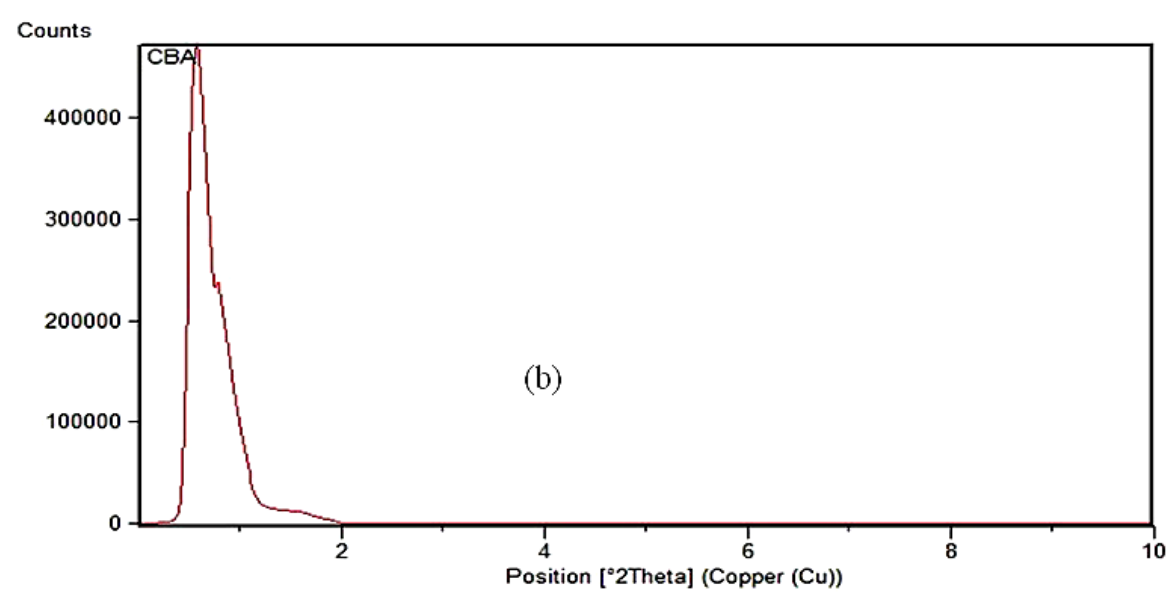


Figure 3. Low-angle X-ray diffractogram of (a) uncalcined and (b) calcined samples.

Figure 4 illustrates the SEM micrographs of the uncalcined and calcined samples at different magnifications. The SEM analysis revealed the surface morphologies of the synthesised mesoporous silica samples, with the calcination process notably affecting their structure [14]. The high-resolution image in Figure 4(b) shows mesoporous cubic crystals, with silica and alumina particles arranged

in a plate-like structure, some sliding over one another [15]. In the SEM images (c, d), most particles appeared nearly spherical, although agglomerates were visible after calcination. The calcined samples exhibited an agglomerate morphology with larger, uniformly distributed pores, which is a characteristic of MCM-41-type mesoporous silica [16].

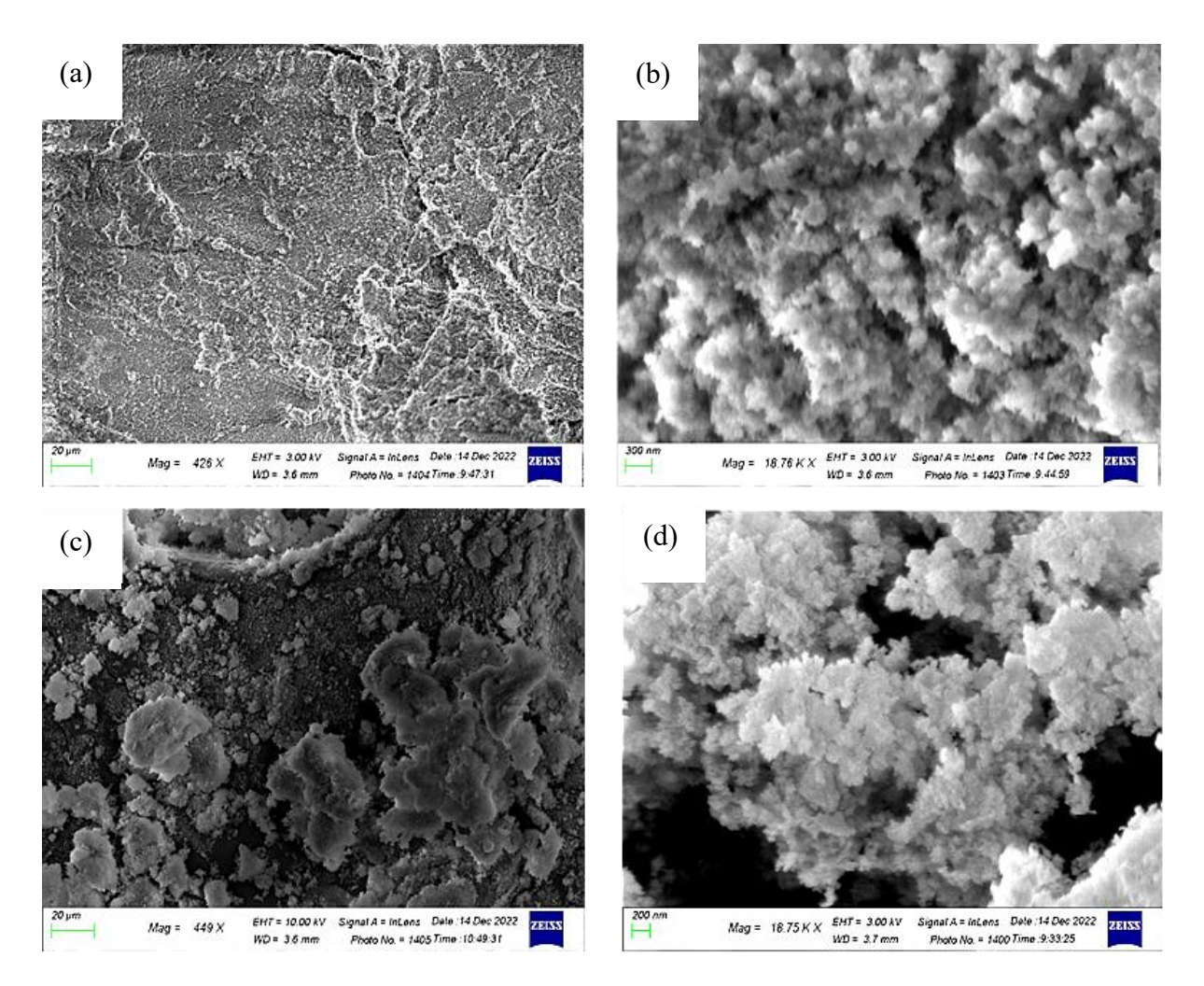


Figure 4. SEM micrograph of (a, b) uncalcined and (c, d) calcined samples.

Table 2 presents the elements identified in the synthesised mesoporous silica materials. The EDX results revealed that the uncalcined sample contained 53.17% oxygen and 46.83% silicon. For the calcined sample, the percentage of oxygen decreased to 25.19%, while the silicon content increased to 74.81%. An uncalcined sample typically retains a higher proportion of water and organic impurities, which can affect its overall composition. For instance, EDX analysis of uncalcined silica often shows a higher oxygen content relative to silicon due to the presence of hydroxyl groups and moisture. Calcination, which involves heating the silica material at high temperatures, removes water and organic impurities, thus enhancing the purity of the silica. This results in a higher silicon content than oxygen [17]. The calcination process also typically leads to an increase in the weight

percentage of silicon while decreasing that of oxygen. The finding is supported by physical sorption analysis, which shows a consistent process of adsorption and desorption [18].

The structural changes observed after calcination, as evidenced by the FTIR, XRD, and SEM-EDX analyses, are expected to influence the adsorption behaviour of the mesoporous silica. The removal of surfactants, improved silica purity, and the development of an ordered pore structure with increased crystallinity suggest better accessibility of active sites and enhanced pore connectivity [19]. These features are anticipated to facilitate more effective adsorption of dye molecules. The relationship between these structural properties and erythrosine adsorption is further discussed in the following section.

Table 2. SEM-EDX of Elements.

Sample	Elements	Weight (%)	Atomic (%)
Uncalcined	Oxygen	53.17	66.59
	Silicon	46.83	33.41
Calcined	Oxygen	25.19	37.15
	Silicon	74.81	62.85

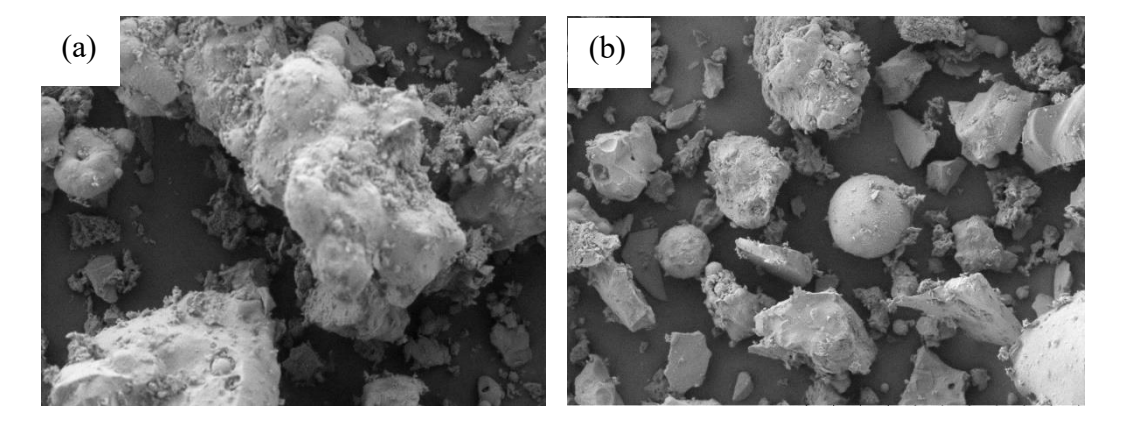


Figure 5. Morphology structure of the sample (a) before dye adsorption, (b) after dye adsorption.

Erythrosine Adsorption Study

The SEM-EDX images provide a comparative analysis of the surface morphology of synthesised mesoporous silica materials before and after the adsorption of erythrosine dye (Figure 5). The material before adsorption (see Figure 5(a)) has a rougher, uneven surface with distinct textural features. The greater surface area and more accessible active sites for binding dye molecules

like erythrosine indicate that the material is in its activated state and ideal for adsorption. In contrast, Figure 5(b) shows the material after adsorption, where the particles appear smoother and more aggregated. This change in morphology is attributed to the deposition of dye molecules on the surface, which may have reduced the porosity. The smoother surface after adsorption confirms the interaction between the adsorbent and the dye, hence supporting the adsorption process.

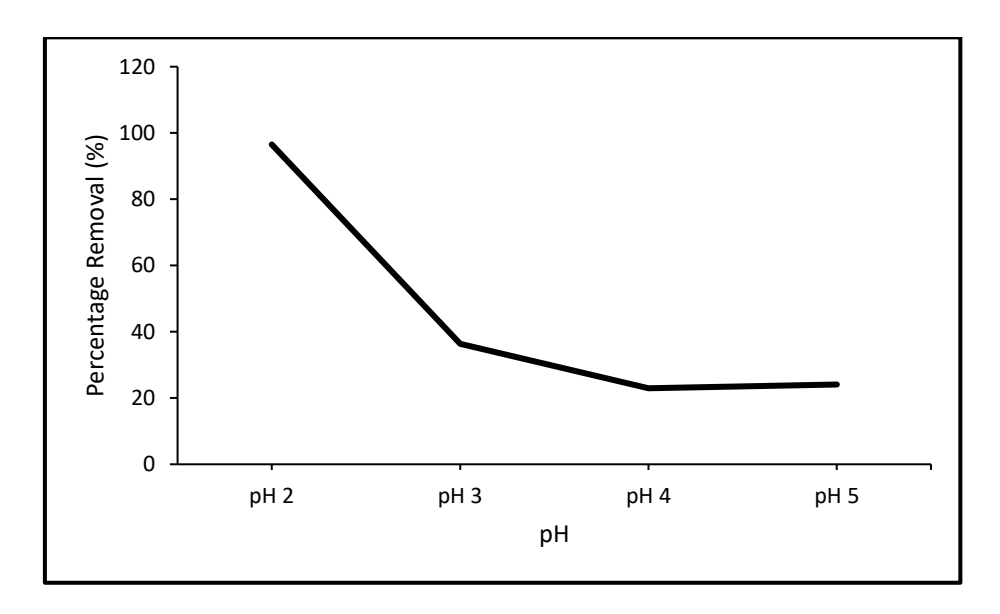


Figure 6. Graph of the effect of pH against percentage removal

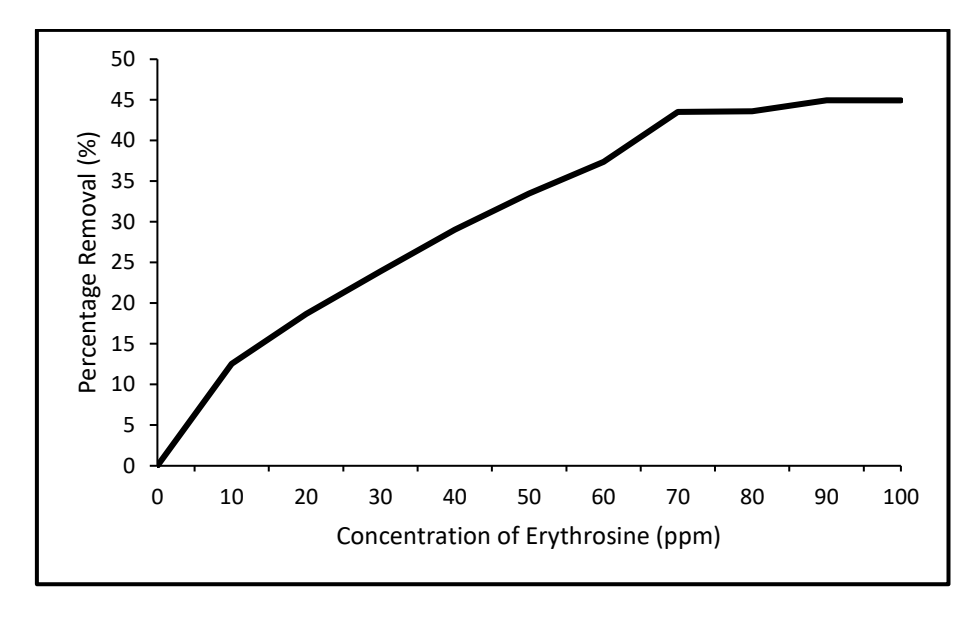


Figure 7. Graph of concentration of erythrosine (ppm) against percentage removal.

Figure 6 shows the percentage removal as a function of pH. The percentage removal is highest, approaching 100%, at pH 2. Dye removal decreases as the pH increases up to 4, after which it remains constant. At low pH, the adsorbent becomes more protonated and gains more hydrogen ions (H⁺) that neutralise its negative charges, making it positively charged. This facilitates the diffusion of dye molecules to active sites, subsequently increasing adsorption efficiency. Since erythrosine is an anionic dye, it is strongly attracted to the positively charged

surface through electrostatic forces. As pH rises, the adsorbent surface loses protons, reducing its positive charge and adsorption capacity. At higher pH, the surface may even become negatively charged and repel the dye molecules [20]. These factors explain the decrease in adsorption capacity with increasing pH. A similar pH-dependent trend was reported in a study using copper oxide nanoparticles, which showed maximum erythrosine removal of 93.68% at pH 2, thus highlighting the favourable adsorption of the dye under acidic conditions [21].

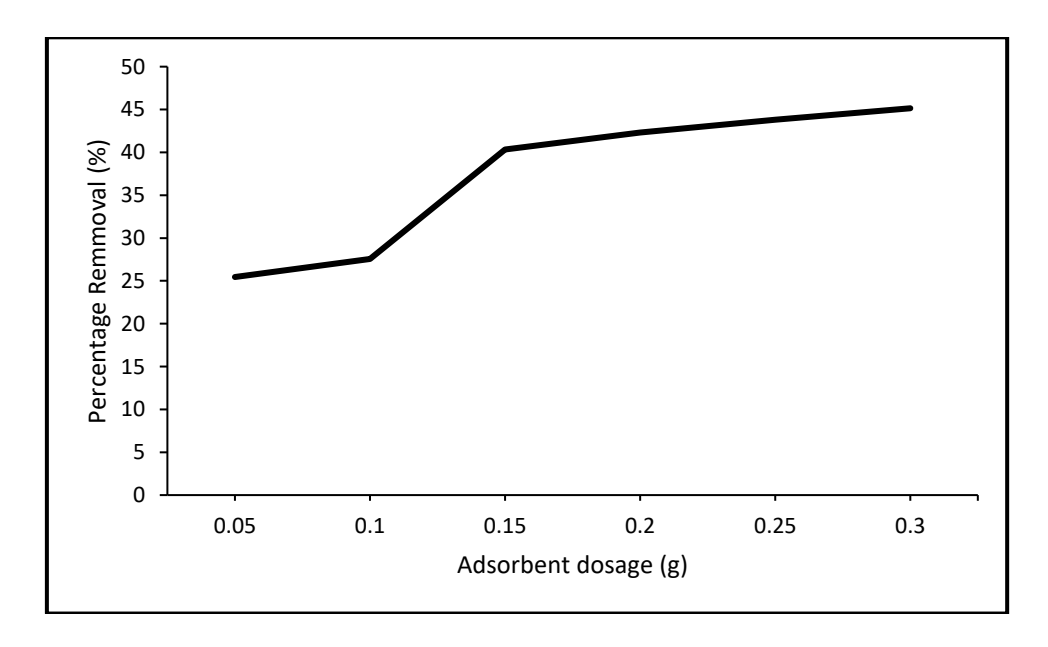


Figure 8. Graph of adsorbent dosage (g) against percentage removal.

25 Afifah Athirah Saini, Anis Haziqah Mohd Yusof, Fatin Nur Athirah Mohmad Rosli, Muhamad Hafiz Zulkafli, Mursyida Mohd Dakroh, Maryam Husin and Hamizah Md Rasid Removal of Erythrosine Dye from Aqueous Solutions using Mesoporous Silica Synthesised from Coal Bottom Ash

The adsorption process was further examined using different concentrations of erythrosine to determine the percentage removal. As shown in Figure 7, the percentage removal increased with erythrosine concentrations. The removal steadily rose to about 45% as the concentration increased from 10 to 70 ppm, indicating that the adsorbent had sufficient active sites to bind with dye molecules at lower concentrations. However, the percentage removal plateaued between 45% and 50% as the concentration exceeded 70 ppm, suggesting that the adsorbent had reached its adsorption capacity and most active sites were occupied. Therefore, further increases in dye concentration result in minimal improvements in removal efficiency.

The experiment was further conducted with different dosages of adsorbent to remove erythrosine from solutions, with a concentration of 40 ppm. As shown in Figure 8, the percentage removal increased with adsorbent dosage. The removal rose sharply from 25% at 0.05 g to 45% at 0.15 g, reaching a maximum of nearly 50% at 0.3 g. Beyond this point, the percentage removal plateaued, indicating that most erythrosine molecules had been adsorbed and further increases in dosage would have little effect. This plateau suggests that equilibrium has been reached, and the decreasing adsorption efficiency at higher dosages may be due to saturation of active sites, adsorbent particle overlap, or dilution effects where fewer dye molecules are available for adsorption [22-23].

CONCLUSION

In this study, mesoporous silica materials were successfully synthesised from coal bottom ash using the hydrothermal method. Characterisation via FTIR, XRD, and SEM-EDX confirmed the successful synthesis. The FTIR spectra showed the presence of surface hydroxyl groups and symmetric Si-O stretching, while the XRD patterns revealed an ordered pore structure. EDX analysis indicated that the synthesised material was primarily composed of silica and oxygen, with a uniform composition. The synthesised mesoporous silica demonstrated effective erythrosine removal from aqueous solutions. Maximum adsorption (~100% removal) occurred at pH 2. Adsorption efficiency increased with higher dye concentrations due to the availability of active sites. The removal efficiency also improved with increasing adsorbent dosage, but plateaued after saturation, as particle aggregation reduced the effective surface area.

ACKNOWLEDGEMENTS

The authors would like to express their gratitude to the Ministry of Higher Education (MOHE) Malaysia for funding this work, which was conducted at the Faculty of Applied Sciences, Universiti Teknologi MARA, Malaysia. This research was

supported by the Fundamental Research Grant Scheme No. FRGS/2/2013/SG01/UITM/03/1 (600-RMI/FRGS 5/3 (59/2013). Similar appreciation is extended to the Tanjung Bin Power Plant, Pontian, Johor for supplying the coal bottom ash.

REFERENCES

- Zhou, H., Bhattarai, R., Li, Y., Si, B., Dong, X., Wang, T. and Yao, Z. (2022) Towards Sustainable Coal Industry: Turning Coal Bottom Ash into Wealth. Science of the Total Environment, 804, 149985.
- 2. Ramzi, N. I. R., Shahidan, S., Maarof, M. Z. and Ali, N. (2016) Physical and Chemical Properties of Coal Bottom Ash (CBA) from Tanjung Bin Power Plant. *IOP Conference Series: Materials Science and Engineering*, **160**, 012056.
- 3. Rafieizonooz, M., Mirza, J., Salim, M. R., Hussin, M. W. and Khankhaje, E. (2016) Investigation of coal Bottom Ash and Fly Ash in Concrete as a Replacement for Sand and Cement. *Construction and Building Materials*, **116**, 15–24.
- 4. Marto, A. and Tan, C. S. (2016) Properties of Coal Bottom Ash from Power Plants in Malaysia and Its Suitability as Geotechnical Engineering Material. *Jurnal Teknologi*, **78(8–5)**, 1–10.
- 5. Ab Rahman, N. B., Md Rasid, H., Mohammad Hassan, H. and Noor Jalil, M. (2016) Synthesis and Characterization of Mesoporous Silica MCM-41 and SBA-15 from Power Plant Bottom Ash. *Malaysian Journal of Analytical Science*, **20(3)**, 539–545.
- 6. Liu, Z. S., Li, W. K. and Huang, C. Y. (2014) Synthesis of Mesoporous Silica Materials from Municipal Solid Waste Incinerator Bottom Ash. *Waste Management*, **34(5)**, 893–900.
- Gupta, R., Ranjan, S., Yadav, A., Verma, B., Malhotra, K., Madan, M., Chopra, O., Jain, S., Gupta, S., Joshi, A., Bhasin, C. and Mudgal, P. (2019) Toxic Effects of Food Colorants Erythrosine and Tartrazine on Zebrafish Embryo Development. Current Research in Nutrition and Food Science, 7(3), 876–885.
- 8. Chandrasekar, G., You, K. S., Ahn, J. -W. and Ahn, W. -S. (2008) Synthesis of Hexagonal and Cubic Mesoporous Silica using Power Plant Bottom Ash. *Microporous and Mesoporous Materials*, **111(1-3)**, 455–462.
- de Oliveira, F. F., Moura, K. O., Costa, L. S., Vidal, C. B., Loiola, A. R. and do Nascimento, R. F. (2020) Reactive Adsorption of Parabens on Synthesized Micro- and Mesoporous Silica from

- 26 Afifah Athirah Saini, Anis Haziqah Mohd Yusof, Fatin Nur Athirah Mohmad Rosli, Muhamad Hafiz Zulkafli, Mursyida Mohd Dakroh, Maryam Husin and Hamizah Md Rasid
 - Coal Fly Ash: pH Effect on the Modification Process. ACS Omega, 5(7), 3346–3357.
- Yahya, A. A., Ali, N., Kamal, N. L. M., Shahidan, S., Beddu, S., Nuruddin, M. F. and Shafiq, N. (2017) Reducing Heavy Metal Element from Coal Bottom Ash by using Citric Acid Leaching Treatment. MATEC Web of Conferences, 103, 01004.
- Niculescu, V. C., Miricioiu, M., Enache, S., Constantinescu, M., Bucura, F. and David, E. (2019) Optimized Method for Producing Mesoporous Silica from Incineration Ash, Progress of Cryogenics and Isotopes Separation, 22(2), 65-76.
- 12. Sorcar, S. and Saini, K. K. (2014) Synthesis of Highly Ordered Silica Microspheres with Uniform Nanosized Pores by Sol Gel Route. *Advanced Porous Materials*, **2(1)**, 42–47.
- 13. Nagappan, S., Jeon, Y., Park, S. S. and Ha, C. S. (2019) Hexadecyltrimethylammonium Bromide Surfactant-Supported Silica Material for the Effective Adsorption of Metanil Yellow Dye. *ACS Omega*, **4(5)**, 8548–8558.
- Şahin, Y. (2021) Understanding the Effect of Calcination Process on the Mesoporous MCM-41 Material Morphology. *Journal of the Turkish Chemical Society*, 4(2), 27–32.
- Iqra, J., Faryal, M., Uzaira, R. and Noshaba, T. (2014) Preparation of Zeolite from Incinerator Ash and its Application for the Remediation of Selected Inorganic Pollutants: A greener Approach. *IOP Conference Series: Materials Science and Engineering*, 60, 012060.
- Miricioiu, M. G., Niculescu, V. -C., Filote, C., Raboaca, M. S. and Nechifor, G. (2021) Coal Fly Ash Derived Silica Nanomaterial for MMMs—Application in CO₂/CH₄ Separation. Membranes, 11(2), 78.

- Removal of Erythrosine Dye from Aqueous Solutions using Mesoporous Silica Synthesised from Coal Bottom Ash
- 17. Imoisili, P. E., Ukoba, K. and Jen, T. (2020) Synthesis and Characterization of Amorphous Mesoporous Silica from Palm Kernel Shell Ash. *Boletín De La Sociedad Española De Cerámica Y Vidrio*, **59(4)**, 159–164.
- Thahir, R., Wahab, A., Nafie, N. and Raya, I. (2019) Synthesis of High Surface Area Mesoporous Silica SBA-15 by Adjusting Hydrothermal Treatment Time and the Amount of Polyvinyl Alcohol. Open Chemistry, 17(1), 963-971.
- Zhou, W., Sun, F., Pan, K., Tian, G., Jiang, B., Ren, Z., Tian, C. and Fu, H. (2011) Well-ordered Large-pore Mesoporous Anatase TiO₂ with Remarkably High Thermal Stability and Improved Crystallinity: Preparation, Characterization, and Photocatalytic Performance. Advanced Functional Materials, 21(10), 1922–1930.
- Litefti, K., Freire, M. S., Stitou, M. and González-Álvarez, J. (2019) Adsorption of an Anionic Dye (Congo Red) from Aqueous Solutions by Pine Bark. Scientific Reports, 9(1), 16530.
- Hosny, N. M., Gomaa, I. and Elmahgary, M. G. (2023) Adsorption of Polluted Dyes from Water by Transition Metal Oxides: A Review. Applied Surface Science Advances, 15, 100395.
- Rápó, E. and Tonk, S. (2021) Factors Affecting Synthetic Dye Adsorption; Desorption Studies: A Review of Results from the Last Five Years (2017–2021). *Molecules*, 26(17), 5419.
- Binaeian, E., Babaee Zadvarzi, S. and Yuan, D. (2020) Anionic Dye Uptake via Composite using Chitosan-Polyacrylamide Hydrogel as Matrix Containing TiO₂ Nanoparticles; Comprehensive Adsorption Studies. *International Journal of Biological Macromolecules*, 162, 150–162.